

Indirect measurements of the $\tilde{\tau}-\tilde{\chi}_1^0$ mass difference and $M_{\tilde{g}}$ in the co-annihilation region of mSUGRA models at the LHC

Richard Arnowitt^a, Adam Aurisano^a, Bhaskar Dutta^{a,*}, Teruki Kamon^a, Nikolay Kolev^b,
Paul Simeon^a, David Toback^a, Peter Wagner^a

^a Department of Physics, Texas A&M University, College Station, TX 77843-4242, USA

^b Department of Physics, University of Regina, Regina, SK S4S 0A2, Canada

Received 28 August 2006; received in revised form 13 March 2007; accepted 16 March 2007

Available online 4 April 2007

Editor: M. Cvetič

Abstract

We study the prospects for the measurement of the $\tilde{\tau}-\tilde{\chi}_1^0$ mass difference (ΔM) and the \tilde{g} mass ($M_{\tilde{g}}$) in the supersymmetric co-annihilation region of mSUGRA at the LHC using tau leptons. Recent WMAP measurements of the amount of cold dark matter and previous accelerator experiments favor the co-annihilation region of mSUGRA, characterized by a small ΔM (5–15 GeV). Focusing on taus from $\tilde{\chi}_2^0 \rightarrow \tau\tilde{\tau} \rightarrow \tau\tau\tilde{\chi}_1^0$ decays in \tilde{g} and \tilde{q} production, we consider inclusive $3\tau + \text{jet} + \cancel{E}_T$ production, with two τ 's above a high E_T threshold and a third τ above a lower threshold. Two observables, the number of opposite-signed τ pairs minus the number of like-signed τ pairs, and the peak of the di-tau invariant mass distribution, allow for the simultaneous determination of ΔM and $M_{\tilde{g}}$ for $\Delta M \gtrsim 6$ GeV. For example, for $\Delta M = 9$ GeV and $M_{\tilde{g}} = 850$ GeV with 30 fb^{-1} of data, we can measure ΔM to 15% and $M_{\tilde{g}}$ to 6%.
© 2007 Elsevier B.V. All rights reserved.

1. Introduction

Supersymmetry (SUSY), a symmetry between fermions and bosons, allows for the construction of models that link a wide range of physical phenomena. While initially proposed on aesthetic grounds, SUSY also allows for cancellation of the quadratic Higgs divergence and, hence, opens the window for consistent model building up to the grand unification (GUT) or Planck scales. The extension of supersymmetry to a local gauge theory, supergravity [1], led to the development of GUT models [2,3] giving a description of physics from the GUT scale down to the electroweak scale, in addition to incorporating the successes of the Standard Model (SM). This idea of SUSY grand unification has been confirmed in the LEP data [4]. Additionally, SUSY models with R-parity conservation automatically give rise to a cold dark matter candidate,

the lightest neutralino, $\tilde{\chi}_1^0$. Because these models are consistent to very high energies, they provide descriptions of the early universe that deeply link particle physics and cosmology. Detailed theoretical calculations [5] confirm that GUT models can account for the experimentally observed dark matter abundance [6].

There is good reason to believe that SUSY can be discovered at the Large Hadron Collider (LHC) and that it may be possible to determine its parameters with enough precision to distinguish among SUSY models that correctly predict the dark matter content of the universe. While the ideal is to study the prospects of measuring SUSY in as general a way as possible, we consider mSUGRA [2] here, a commonly studied model, for concreteness. In mSUGRA, four parameters and one sign determine all the masses and couplings: m_0 , the universal scalar soft breaking mass at M_{GUT} ; $m_{1/2}$, the universal gaugino mass at M_{GUT} ; A_0 , the universal cubic soft breaking parameter at M_{GUT} ; $\tan\beta = \langle H_1 \rangle / \langle H_2 \rangle$, where $\langle H_{1(2)} \rangle$ is the Higgs vacuum expectation value which gives rise to the up (down)

* Corresponding author.

E-mail address: dutta@physics.tamu.edu (B. Dutta).

quark masses; and the sign of μ , where μ is the coefficient of the quadratic term of the superpotential, $W = \mu H_1 H_2$. While mSUGRA is the simplest supergravity GUT model, as noted below, the techniques described here can be applied to a relatively wide class of models.

While production and annihilation rates of $\tilde{\chi}_1^0$ help determine the dark matter content of the early universe, existing constraints can help constrain the available parameter space. Dark matter abundance measurements and accelerator data point to three different types of regions [5]: (1) the $\tilde{\tau}-\tilde{\chi}_1^0$ co-annihilation region [7]¹ where $\Delta M \equiv M_{\tilde{\tau}} - M_{\tilde{\chi}_1^0}$ is small, ($\Delta M \sim 5-15$ GeV) which reduces the $\tilde{\chi}_1^0$ density by allowing $\tilde{\tau}-\tilde{\chi}_1^0$ co-annihilation into SM particles, (2) the focus point region where the $\tilde{\chi}_1^0$ has a large higgsino component, and (3) the scalar Higgs annihilation funnel region. A bulk region is also allowed by dark matter constraints, but it is largely excluded by other constraints. A collection of other constraints suggests that, of these regions, the co-annihilation region is particularly important. They include the light Higgs and lightest chargino mass bounds from LEP [8], the $b \rightarrow s\gamma$ branching ratio bound [9], and the 3.4σ deviation from the SM expectation of the anomalous muon magnetic moment from the muon $g-2$ Collaboration [10]. If the anomalous muon magnetic moment deviation is proven, mostly the co-annihilation region will be allowed. Since, in principle, $M_{\tilde{\tau}}$ and $M_{\tilde{\chi}_1^0}$ can separately range from 100 GeV into the TeV domain, if this striking smallness of ΔM were found at the LHC, it would be a strong indirect indication that the $\tilde{\chi}_1^0$ is the astronomical dark matter particle. We also note that many other SUGRA models have a co-annihilation region since the possibility of co-annihilation does not depend on either the gaugino or squark mass universality of mSUGRA (though, constraints do not necessarily exist to uniquely select out the co-annihilation region). Thus, investigating this region has applicability beyond mSUGRA.

Measuring the masses of the superparticles in the co-annihilation region is difficult both because there are τ 's in the final state in general, and because the τ 's from $\tilde{\tau} \rightarrow \tau \tilde{\chi}_1^0$ decays are low energy in particular. One study showed that the co-annihilation region can be established at a high energy e^+e^- International Linear Collider machine, and that a small ΔM can be measured with 10% precision [11]. However, prospects for the LHC are more interesting as it's data should be available much sooner. While general methods for high $\tan\beta$ measurements using di-tau final states are well established [12], an analysis that takes into account the small ΔM of the co-annihilation region has shown that with a $2\tau + 2\text{jet} + \cancel{E}_T$ data set a ΔM measurement precision of 18% is possible with a luminosity of 10 fb^{-1} at the LHC [13]. However, that analysis requires that an independent gluino mass measurement exists at the 5% level.

The two proposed gluino mass measurement methods for high $\tan\beta$ described in Ref. [12] require modification and/or

high luminosity to be used if the co-annihilation region is realized in nature. The first uses an M_{eff} observable, constructed out of the 4 highest energy jets and \cancel{E}_T from squark and gluino decays. In the co-annihilation region this may not produce the stated 10% uncertainty because two out of the four jets can easily be from hadronic tau decays. In this case the neutrinos arising from their decays could add uncertainty to the measurement both as lost energy and more variation in the observed energy; a study on how to properly modify the method to take these effect into account is underway. The second method is to measure the masses using fully reconstructed events in the $2b + 2\tau + \text{jets} + \cancel{E}_T$ final state. The prospects for that analysis use $\Delta M \sim 50$ GeV which gives larger average energies for the final state taus, thus requiring high luminosity for similar precision at low ΔM . Similarly, the production cross sections considered there for $M_{\tilde{g}} = 550$ GeV would be significantly lower for the larger mass gluinos of the co-annihilation region (~ 850 GeV). Thus, while a gluino mass measurement with an accuracy of 10% or better can be achieved, it is unlikely with either method with $10-30 \text{ fb}^{-1}$ of luminosity.

We show below that it should be possible to measure $M_{\tilde{g}}$ in the co-annihilation region to $\simeq (5-10)\%$ accuracy. This measurement, however, makes use of the gaugino universality of mSUGRA at M_{GUT} . If in addition a measurement of $M_{\tilde{g}}$ (independent of gaugino universality) can be made, the two measurements would be complementary. Thus, if they agreed, this would verify the gaugino universality of mSUGRA, while if they disagreed it would determine the amount of non-universality in the correct model. In either case, the existence of both measurements of $M_{\tilde{g}}$ would help shed light on the nature of GUT scale physics.

In this Letter, we describe new techniques as a part of a program that would establish that the co-annihilation region is realized in nature at the LHC, and detail the prospects of measuring ΔM and $M_{\tilde{g}}$ simultaneously. Here, we assume that there is no dimuon and/or dielectron excess observed at the LHC, indicating high $\tan\beta$ (the domination of taus in the final states starts from $\tan\beta = 10$ for the co-annihilation region). We consider an mSUGRA scenario in the co-annihilation region with $\tan\beta = 40$ GeV, $A_0 = 0$, and $\mu > 0$, but we allow m_0 and $m_{1/2}$ to vary such that $\Delta M < 20$ GeV. In our calculations we vary m_0 in the range 205 to 230 GeV and $m_{1/2}$ in the range 310 to 415 GeV to study the effects of different values of ΔM and $M_{\tilde{g}}$. In each case we utilize the universal gaugino mass relations of SUGRA models. In Table 1 we show the SUSY parameters for our reference point $M_{\tilde{g}} = 850$ GeV, $\Delta M = 9$ GeV. In Section 2, we describe the requirements to select inclusive $3\tau + \text{jet} + \cancel{E}_T$ events. In particular, we motivate our selection criteria and describe the mass and counting observables. In this section, it will become clear that a primary experimental requirement for this analysis to be realized in practice is the efficiency to identify taus with E_T as low as 20 GeV. In Section 3, we discuss a method to use both observables to simultaneously determine both ΔM and $M_{\tilde{g}}$. Conclusions are given in Section 4.

¹ Note that the notation $\tilde{\tau}$ here refers to the lighter of the two supersymmetric tau mass eigenstates.

Table 1

Masses (in GeV) of the SUSY particles for our reference point for $m_{1/2} = 360$ GeV, $m_0 = 211.6$ GeV, $\tan\beta = 40$, $\mu > 0$, and $A_0 = 0$

\tilde{g}	\tilde{q}_{uL}	\tilde{q}_{uR}	\tilde{t}_2	\tilde{t}_1	$\tilde{\tau}_2$	\tilde{e}_L	$\tilde{\chi}_2^0$	\tilde{e}_R	$\tilde{\tau}_1$	$\tilde{\chi}_1^0$	$\Delta M (\equiv M_{\tilde{\tau}_1} - M_{\tilde{\chi}_1^0})$
850	764	741	742	574	334	324	267	253	153	144	9

2. Detecting a SUSY signal in the co-annihilation region using the 3τ final state

The primary SUSY production processes at the LHC are $pp \rightarrow \tilde{q}\tilde{g}, \tilde{q}\tilde{q}, \tilde{g}\tilde{g}$. In each case they decay via $\tilde{q} \rightarrow q'\tilde{\chi}_1^\pm$ or $q\tilde{\chi}_2^0$ (or $\tilde{q}_R \rightarrow q\tilde{\chi}_1^0$); $\tilde{g} \rightarrow q\tilde{q}'\tilde{\chi}_1^\pm$ or $q\tilde{q}\tilde{\chi}_2^0$; and $\tilde{g} \rightarrow \tilde{t}\tilde{t}_1$ or $\tilde{b}\tilde{b}_1$ and their charge conjugate states, generally producing high E_T jets and gaugino pairs. Since we are interested in measuring both the $\tilde{\tau}-\tilde{\chi}_1^0$ mass difference and the gluino mass simultaneously and unambiguously, we investigate the $\tilde{\tau} \rightarrow \tau\tilde{\chi}_1^0$ decay. The branching ratio of $\tilde{\chi}_2^0 \rightarrow \tau\tilde{\tau}$ is about 97% for our parameter space and is dominant even for large $m_{1/2}$ in the entire co-annihilation region. The same is true for the $\tilde{\chi}_1^\pm \rightarrow \nu\tilde{\tau}$ decay mode. Therefore, the $\tilde{\tau} \rightarrow \tau\tilde{\chi}_1^0$ decay is present in events with $\tilde{\chi}_2^0\tilde{\chi}_2^0$, $\tilde{\chi}_1^\pm\tilde{\chi}_2^0$, $\tilde{\chi}_1^+\tilde{\chi}_1^-$, and $\tilde{\chi}_2^0\tilde{\chi}_1^0$ pairs. The decays of $\tilde{\chi}_1^\pm$ particles are less desirable than the decays of $\tilde{\chi}_2^0$ particles even though the decay of squarks and gluinos have a larger branching fraction to $\tilde{\chi}_1^\pm$'s than to $\tilde{\chi}_2^0$'s. The reason is that $\tilde{\chi}_2^0$ decays produce a correlated pair of one high energy tau from $\tilde{\chi}_2^0 \rightarrow \tau\tilde{\tau}$ and one low energy tau from $\tilde{\tau} \rightarrow \tau\tilde{\chi}_1^0$ from which we can extract kinematic information $\tilde{\chi}_2^0 \rightarrow \tau\tilde{\tau} \rightarrow \tau\tau\tilde{\chi}_1^0$, whereas $\tilde{\chi}_1^\pm$ decays only produce a single low energy tau via $\tilde{\chi}_1^\pm \rightarrow \tilde{\tau}\nu \rightarrow \tau\nu\tilde{\chi}_1^0$. Therefore, we focus on isolating a pair of hadronically-decaying τ 's from $\tilde{\chi}_2^0$ decays.

The $\tilde{\chi}_2^0\tilde{\chi}_2^0$, $\tilde{\chi}_2^0\tilde{\chi}_1^\pm$, and $\tilde{\chi}_2^0\tilde{\chi}_1^0$ channels each contain a $\tilde{\chi}_2^0$ decay chain and lead to final states with four, three, and two τ 's respectively, each with experimental advantages and disadvantages. The 4τ final state is the cleanest in that it has very small background, especially from SM sources; the disadvantage is that it has small acceptance for reconstructing all four τ 's. The 2τ final state is the inverse case; as discussed in [13], there are significant backgrounds that must be dealt with, but the acceptance is large because a 2τ signature allows all three channels. The 3τ analysis provides a compromise. We study it here as an alternative to the 2τ case since the possibility exists that the backgrounds for the 2τ case are underestimated. It will require actual data to determine which analysis performs better or if both are needed. It may be that the two analyses can be combined to provide additional information; this is under study.

The 3τ final state contains both SM and SUSY backgrounds. The primary SM background is $t\bar{t}$ production which produces two τ 's, one from each $t \rightarrow Wb \rightarrow \tau\nu b$, and a third τ coming from either a bottom decay (expected to be non-isolated). There are two major sources of SUSY background: real τ 's from decays of $\tilde{\chi}_1^\pm$'s or \tilde{t}_1 's. Both of these can produce low or high energy τ 's, but they are uncorrelated and, as we will see, can be separated statistically from $\tilde{\chi}_2^0$ decays by opposite-signed/like-signed subtraction ($OS-LS$). In addition, jets faking τ 's leads to

additional backgrounds due to both SM and SUSY production, but these can be handled similarly.

Our primary method for separating τ pairs from $\tilde{\chi}_2^0$ decays from other sources is to use the standard $OS-LS$ technique, which is used in other analyses [13,14]. To do this in our case we order the taus by E_T ($E_T^{\tau_1} > E_T^{\tau_2} > E_T^{\tau_3}$) and only consider the pairs $\tau_1\tau_3$ and $\tau_2\tau_3$. For illustration, consider a $\tilde{\chi}_2^0\tilde{\chi}_2^0$ event. We expect τ_1 and τ_2 to be from the two $\tilde{\chi}_2^0 \rightarrow \tau\tilde{\tau}$ decays because the mass difference between the $\tilde{\chi}_2^0$ and the $\tilde{\tau}$ is large ($M_{\tilde{\chi}_2^0} \approx 267$ GeV and $M_{\tilde{\tau}} \approx 153$ GeV), and we expect τ_3 to be from the $\tilde{\tau} \rightarrow \tau\tilde{\chi}_1^0$ decay, since the mass difference between the $\tilde{\tau}$ and the $\tilde{\chi}_1^0$ is small ($M_{\tilde{\chi}_1^0} \approx 144$ GeV). We would expect a τ_4 to also come from the $\tilde{\tau} \rightarrow \tau\tilde{\chi}_1^0$ decay, but we do not consider it in this analysis. Thus, either $\tau_1\tau_3$ or $\tau_2\tau_3$ is from a $\tilde{\chi}_2^0$, so the taus of one pair are correlated and are OS . In the other pair the τ 's are uncorrelated and can be OS or LS with equal probability. Therefore, we subtract the number of observed LS pairs from the number of OS pairs and only use pairs in the kinematically allowed region. As a second example, if our event contains a $\tilde{\chi}_2^0$ and a fake τ from a jet from squark decay, we will have two high energy τ 's and one low energy τ . Again, either the $\tau_1\tau_3$ or $\tau_2\tau_3$ pair is from the $\tilde{\chi}_2^0$, producing a pair that is correlated and OS , while the other pair is uncorrelated and has equal probability of being OS or LS . This same method works for any background where a $\tilde{\chi}_2^0$ is produced along with a τ from another source, for example, from $\tilde{\chi}_1^\pm$ decay.

To generate our signal and backgrounds we simulate our model with all SUSY production using ISAJET [15]. We run the generated particles through a detector simulator, PGS [16], using the CDF parameter file for jet finding, and directly use the visible particle 4-momenta for the tau-jet and electron/muon objects.² Finally, a separate Monte Carlo routine assigns the efficiency for τ 's and fake rate for jets. Based on CDF results we take the τ efficiency to be 50% for τ 's with $E_T > 20$ GeV and the τ fake rate for a jet to be $1.1\% \pm 0.2\%$ [17].³

Based on the simulation expectations, the full set of event selection criteria are listed in Table 2. The first two τ 's have high enough average energies that it is reasonable to cut at $E_T > 40$ GeV and $|\eta| < 2.5$; at this energy, we can expect efficient

² Since we are interested in the peak position of visible di-tau mass distribution, which has large RMS, additional contributions to the measured width from the tau-jet energy resolution are expected to be small. We note that new particle-flow energy measurement techniques are being developed at both ATLAS and CMS which should further improve the energy resolution.

³ At CDF, the jet to τ fake rate is measured to be $1.1 \pm 0.2\%$ for $E^{\text{jet}} \simeq 20$ GeV. As a reasonable assumption for LHC experiments, and for simplicity, we assume a constant fake rate and uncertainty for taus with $E_T > 20$ GeV and $|\eta| < 2.5$.

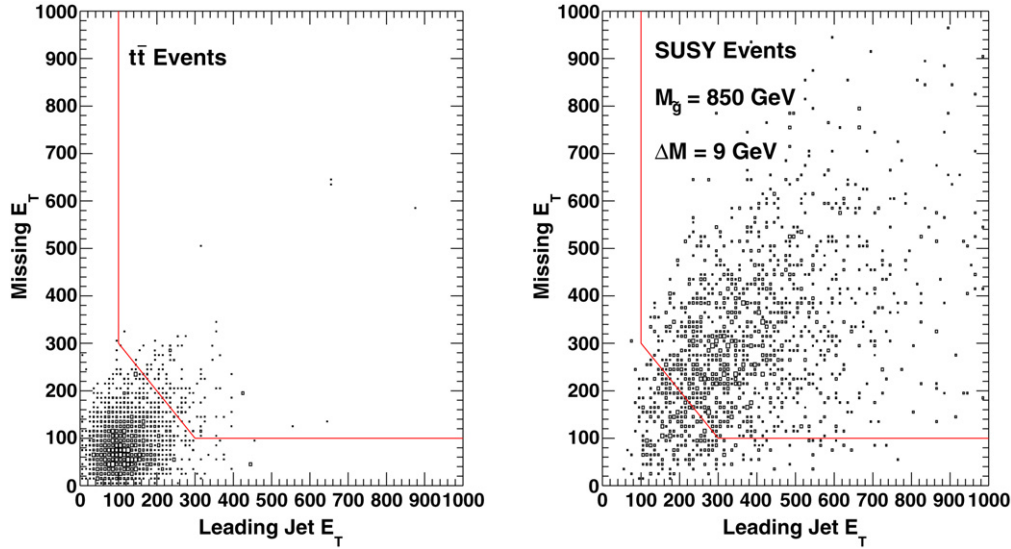


Fig. 1. The correlation between the leading jet E_T and \cancel{E}_T for $t\bar{t}$ (left) and SUSY (right) events after requiring 3 τ 's passing all ID and kinematic cuts in the final state. The SUSY events are for our reference point. The luminosity is arbitrary for SUSY and $t\bar{t}$.

identification. For small ΔM the energy of the third τ , from the $\tilde{\tau} \rightarrow \tau \tilde{\chi}_1^0$ decay, can be very low, often with $E_T \lesssim 15$ GeV. As in [13], we loosen the E_T requirement to 20 GeV as a balance between keeping the maximum number of events while still being in a region of reasonable reproduction of the τ identification capabilities at the LHC detectors.

To further reduce $t\bar{t}$ backgrounds but retain signal we require at least one jet and \cancel{E}_T as shown in Fig. 1. Since we expect all events to end in two $\tilde{\chi}_1^0$'s, we require the \cancel{E}_T to be large. In addition, as previously mentioned, squark decays result in high energy jets. We impose the cuts $\cancel{E}_T > 100$ GeV, $E_T^{\text{jet1}} > 100$ GeV ($|\eta| < 2.5$), and $\cancel{E}_T + E_T^{\text{jet1}} > 400$ GeV. We require a high threshold on the jet and \cancel{E}_T separately to insure that SM events with unusually high jet E_T or \cancel{E}_T have a low likelihood of passing our cuts. This has the further advantage that events passing the cuts should readily pass reasonable jet + \cancel{E}_T triggers envisioned for the LHC.

The invariant mass of the τ pair from the $\tilde{\chi}_2^0$ decay forms a distinct mass distribution and provides excellent rejection against both backgrounds [18]. This can be seen by considering the τ pair in the chain $\tilde{\chi}_2^0 \rightarrow \tau\bar{\tau} \rightarrow \tau\tau\tilde{\chi}_1^0$ in the rest frame of the $\tilde{\chi}_2^0$. In this case, the invariant mass is given by

$$M_{\tau\tau} = M_{\tilde{\chi}_2^0} \sqrt{\frac{1 - \cos\theta}{2}} \sqrt{1 - \frac{M_{\tilde{\tau}}^2}{M_{\tilde{\chi}_2^0}^2}} \sqrt{1 - \frac{M_{\tilde{\chi}_1^0}^2}{M_{\tilde{\tau}}^2}}, \quad (1)$$

where θ is the opening angle between the τ 's; the kinematic endpoint of this distribution corresponds to the $\theta = \pi$ case. Fig. 2 shows the visible di-tau mass, $M_{\tau\tau}^{\text{vis}}$, distribution for SUSY and $t\bar{t}$ production. The endpoint is not visible because of the lost neutrinos, but shows a clear peak that still depends mostly on $M_{\tilde{\chi}_2^0}$, $M_{\tilde{\tau}}$, and $M_{\tilde{\chi}_1^0}$, of which $M_{\tilde{\chi}_2^0}$ and $M_{\tilde{\chi}_1^0}$ are related and depend heavily on $M_{\tilde{g}}$ from the mSUGRA relations. We select τ pairs with $M_{\tau\tau}^{\text{vis}} < 100$ GeV because this is just beyond the endpoint for all ΔM and $M_{\tilde{g}}$ values in our parameter

Table 2

The final selection criteria

3 identified τ candidates with $ \eta < 2.5$ and $E_T > 40, 40$ and 20 GeV respectively
1 jet with $E_T > 100$ GeV and $ \eta < 2.5$
$\cancel{E}_T > 100$ GeV
$\cancel{E}_T + E_T^{\text{jet1}} > 400$ GeV
$M_{\tau\tau}^{\text{vis}} < 100$ GeV where only $\tau_1\tau_3$ and $\tau_2\tau_3$ invariant mass combinations are considered

range. This makes our results less sensitive to the fake rate uncertainty because jets from squarks that fake τ 's tend to have large E_T , which can produce large $M_{\tau\tau}^{\text{vis}}$. In Fig. 2, we also see that the number of events in the peak of the OS distribution in excess above the LS distribution increases as a function ΔM . In addition, the peak position also increases with ΔM [13]. Both these features will be used in the next section. We note that the $t\bar{t}$ distribution also has a peak, but because of the kinematic requirements the event rate is several orders of magnitude less than the SUSY production even without standard isolation cuts, and it is ignored throughout the rest of this Letter. We also note, that as in Ref. [13], lowering the E_T requirement of the τ_3 to 20 GeV is needed for the peak to be visible.

3. Simultaneous measurement of ΔM and $M_{\tilde{g}}$

In this section we define our observables, the number of counts, $N_{\text{OS-LS}}$, and the visible di-tau mass peak position, $M_{\tau\tau}^{\text{peak}}$, and describe their values as a function of both ΔM and $M_{\tilde{g}}$. We then show how these two variables can be used to simultaneously measure both ΔM and $M_{\tilde{g}}$, and compare our ΔM result to previous analyses that assume an independent $M_{\tilde{g}}$ measurement.

The variable $N_{\text{OS-LS}}$ is the number of LS τ pairs subtracted from the number of OS τ pairs passing all the selection requirements in Table 2. Because we expect the τ_3 to come from the

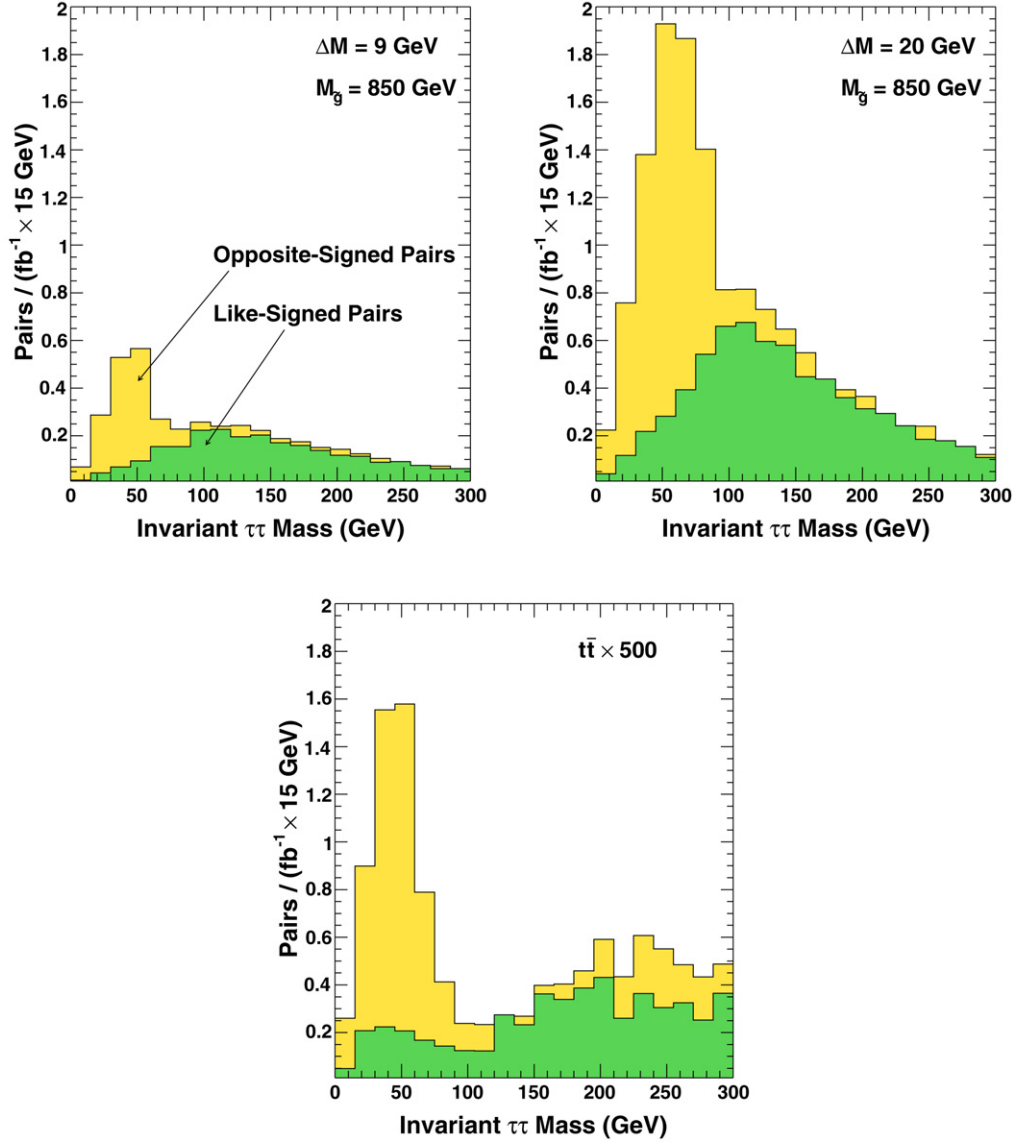


Fig. 2. The visible di-tau mass distribution, $M_{\tau\tau}^{\text{vis}}$, of *OS* and *LS* τ pairs for SUSY events with $\Delta M = 9$ GeV (top left) and $\Delta M = 20$ GeV (top right), and $t\bar{t}$ background (bottom). The *LS* distribution has a characteristic shape of uncorrelated particles. Note that subtracting the *LS* distribution from the *OS* distribution leaves a mass peak due to both τ 's originating from a single $\tilde{\chi}_2^0$ and energy loss from neutrinos. For small ΔM , this peak contains few counts and is centered at low mass, and for large ΔM , this peak contains many counts centered at a higher mass. There is always a kinematical cutoff below ~ 100 GeV. We note that $t\bar{t}$ production also produces a peak, but the event rate is several orders of magnitude smaller than for SUSY production. Therefore, we assume that the SM background is negligible.

$\tilde{\tau} \rightarrow \tau \tilde{\chi}_1^0$ decay, the average E_T of the τ_3 (its probability of having $E_T^{\tau_3} > 20$ GeV), and therefore, $N_{\text{OS-LS}}$ grows with ΔM . Thus, for a known luminosity a measurement of $N_{\text{OS-LS}}$ allows for a determination of ΔM . An increase in $M_{\tilde{g}}$ affects $N_{\text{OS-LS}}$ by decreasing the production rate of gluinos, which decreases the number of $\tilde{\chi}_2^0$ decay chains produced. An increase in $M_{\tilde{g}}$ also increases the boost of the $\tilde{\chi}_2^0$ which increases the number of accepted $\tilde{\chi}_2^0$ decay chains, however, this is a small effect. Though mass changes in squarks and other gauginos also modify both production and boost, the mSUGRA relations relate these directly to ΔM and $M_{\tilde{g}}$. We can write

$$N_{\text{OS-LS}} \propto \sigma(M_{\tilde{g}}) \cdot A(\Delta M, M_{\tilde{g}}), \quad (2)$$

where σ is the total production cross section, A is the ac-

ceptance, and $M_{\tilde{g}}$ effectively provides a scale for the model. Fig. 3 shows $N_{\text{OS-LS}}$ as a function of ΔM and $M_{\tilde{g}}$. We see that $N_{\text{OS-LS}}$ is flat below $\Delta M \sim 5$ GeV and nearly linear above it as a function of ΔM . At low ΔM , the number of τ pairs from $\tilde{\chi}_2^0$ decays goes to zero as none of the τ 's from $\tilde{\tau}$ decay pass the 20 GeV threshold; however, $N_{\text{OS-LS}}$ does not go to zero because of the small SUSY background from stop quark pair production and decay via $\tilde{t}_1 \rightarrow t \tilde{\chi}_i^0 \rightarrow (Wb) \tilde{\chi}_i^0 \rightarrow (\tau\nu) b \tilde{\chi}_i^0$. This background is independent of ΔM , so the small number of events in the very low ΔM region implies that it is negligible. As expected $N_{\text{OS-LS}}$ falls steeply as a function of $M_{\tilde{g}}$.

Two contributions dominate the uncertainty in the $N_{\text{OS-LS}}$ measurement: the statistical uncertainty and the uncertainty in the fake rate. We note that statistical uncertainty is not the usual

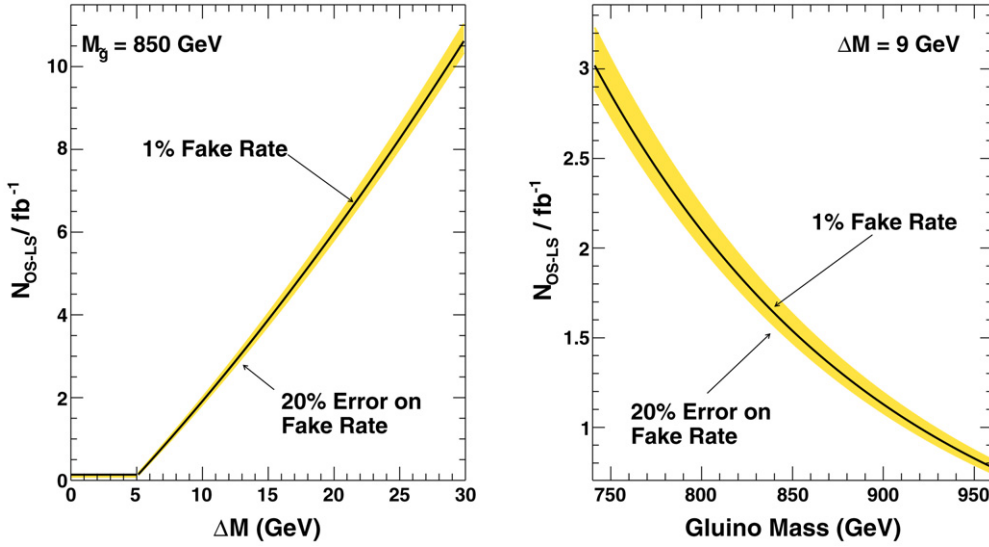


Fig. 3. The left plot shows N_{OS-LS} as a function of ΔM with a 1% fake rate with the shaded band representing the variation due to the 20% systematic uncertainty on the $\tau \rightarrow$ jet fake rate. Below ~ 6 GeV the third τ from $\bar{\tau} \rightarrow \tau \tilde{\chi}_1^0$ is so soft that there is no signal; therefore, counting is dominated by SUSY backgrounds, and the number of counts is flat. Above ~ 6 GeV, the number of counts is nearly linear as a function of ΔM as more and more τ 's from $\bar{\tau} \rightarrow \tau \tilde{\chi}_1^0$ pass the 20 GeV threshold. The right plot shows the relationship between N_{OS-LS} and $M_{\tilde{g}}$ for $\Delta M = 9$ GeV; N_{OS-LS} decreases strongly with increasing $M_{\tilde{g}}$ as larger masses drive down the total production cross section.

\sqrt{N} but, from binomial statistics, $2\sqrt{\frac{N_{OS}N_{LS}}{N_{OS}+N_{LS}}}$ and can be as large as 10% even at 30 fb^{-1} . The 20% uncertainty in the τ fake rate also produces a systematic uncertainty on the true value of N_{OS-LS} . We find the uncertainty due to the fake rate to be small compared to the statistical uncertainty even though $\sim 20\%$ of the N_{OS-LS} event rate is due to events with at least one jet faking a τ . While this may seem puzzling, because of the $OS-LS$ procedure, the additional counts due to the fake rate predominantly come from situations where a τ pair is produced by a $\tilde{\chi}_2^0$ decay, and the first or second τ is due to a jet faking a τ . In this situation, the fake rate is bringing τ pairs from $\tilde{\chi}_2^0$ decay that would have been included in the 2τ analysis is into our sample; therefore, these additional counts do not reduce our sensitivity. Other systematic errors, such as the acceptance and luminosity uncertainties are expected to be small or comparable [19].

We define $M_{\tau\tau}^{\text{peak}}$ as the position of the peak of the visible di-tau invariant mass distribution after the LS distribution is subtracted from the OS distribution. It directly depends on ΔM (as shown in Fig. 2) and indirectly depends on $M_{\tilde{g}}$. The dependences of $M_{\tau\tau}^{\text{peak}}$ enter through Eq. (1) which can be rewritten as

$$M_{\tau\tau}^{\text{peak}} \propto \frac{1}{k} \sqrt{1 - k^2} \sqrt{2\Delta M \cdot M_{\tilde{g}} \cdot k_1}, \quad (3)$$

where we have assumed ΔM is small and $k \simeq M_{\tilde{\chi}_1^0}/M_{\tilde{\chi}_2^0}$ and $k_1 = M_{\tilde{\chi}_1^0}/M_{\tilde{g}}$. Using the mSUGRA relations, $M_{\tilde{g}} \simeq 2.8m_{1/2}$, $M_{\tilde{\chi}_2^0} \simeq 0.8m_{1/2}$, and $M_{\tilde{\chi}_1^0} \simeq 0.4m_{1/2}$, we find $k = 1/2$ and $k_1 = 1/7$. Because of the dependence of the formula on $M_{\tilde{\tau}}$ and $M_{\tilde{\chi}_1^0}^{\text{peak}}$, $M_{\tau\tau}^{\text{peak}}$ rises as a function of ΔM (shown in Fig. 4, top left). As $M_{\tilde{g}}$ changes, so does $M_{\tilde{\chi}_2^0}$ and $M_{\tilde{\chi}_1^0}$, which leads to

$M_{\tau\tau}^{\text{peak}}$ rising as a function of $M_{\tilde{g}}$; this result is shown in Fig. 4 top right.

Due to the large RMS of the distribution, see Fig. 4, the $M_{\tau\tau}^{\text{peak}}$ measurement is dominated by the uncertainty on the number of events in the sample until very high luminosities. The smearing due to jet energy resolution effects and τ polarization uncertainties are small and neglected here (see footnote 2). We take the uncertainty on $M_{\tau\tau}^{\text{peak}}$ to be given by the standard formula, $\sigma_{M_{\tau\tau}^{\text{peak}}} = \text{RMS}/\sqrt{N}$, where \sqrt{N} is the number of counts in the peak (effectively N_{OS-LS}). For $\mathcal{L} = 30 \text{ fb}^{-1}$ and $M_{\tilde{g}} = 850 \text{ GeV}$, we show the statistical uncertainty on $M_{\tau\tau}^{\text{peak}}$ as a band in Fig. 4. The uncertainty due to the fake rate is unmeasurably small compared to the statistical uncertainty, even for large fake rate values, up to 5%. This helps confirm our previous assertion that only τ pairs from a $\tilde{\chi}_2^0$ survive the $OS-LS$ procedure. Pairs not from $\tilde{\chi}_2^0$ decays would have an $M_{\tau\tau}^{\text{peak}}$ that is characteristically shifted. Since this does not happen, even with high fake rates, we conclude that the additional events are from $\tilde{\chi}_2^0 \tilde{\chi}_1^0$ or $\tilde{\chi}_2^0 \tilde{\chi}_1^\pm$ events, which contain τ pairs from a $\tilde{\chi}_2^0$ and an additional τ from a fake or a $\tilde{\chi}_1^\pm$. This is confirmed by the Monte Carlo.

Since N_{OS-LS} and $M_{\tau\tau}^{\text{peak}}$ both depend on ΔM and $M_{\tilde{g}}$ we can invert these dependences to measure ΔM and $M_{\tilde{g}}$ simultaneously. To do this we parameterize N_{OS-LS} and $M_{\tau\tau}^{\text{peak}}$ as functions of ΔM and $M_{\tilde{g}}$. The contours of constant N_{OS-LS} and constant $M_{\tau\tau}^{\text{peak}}$ are shown in Fig. 5 for $\Delta M = 9 \text{ GeV}$ and $M_{\tilde{g}} = 850 \text{ GeV}$. The intersection of these central contours provides the measurement of ΔM and $M_{\tilde{g}}$, and the auxiliary lines, from the expected 1σ uncertainties on N_{OS-LS} and $M_{\tau\tau}^{\text{peak}}$, respectively, determine the 1σ region for ΔM and $M_{\tilde{g}}$. By requiring the measurement of N_{OS-LS} to be statistically significant

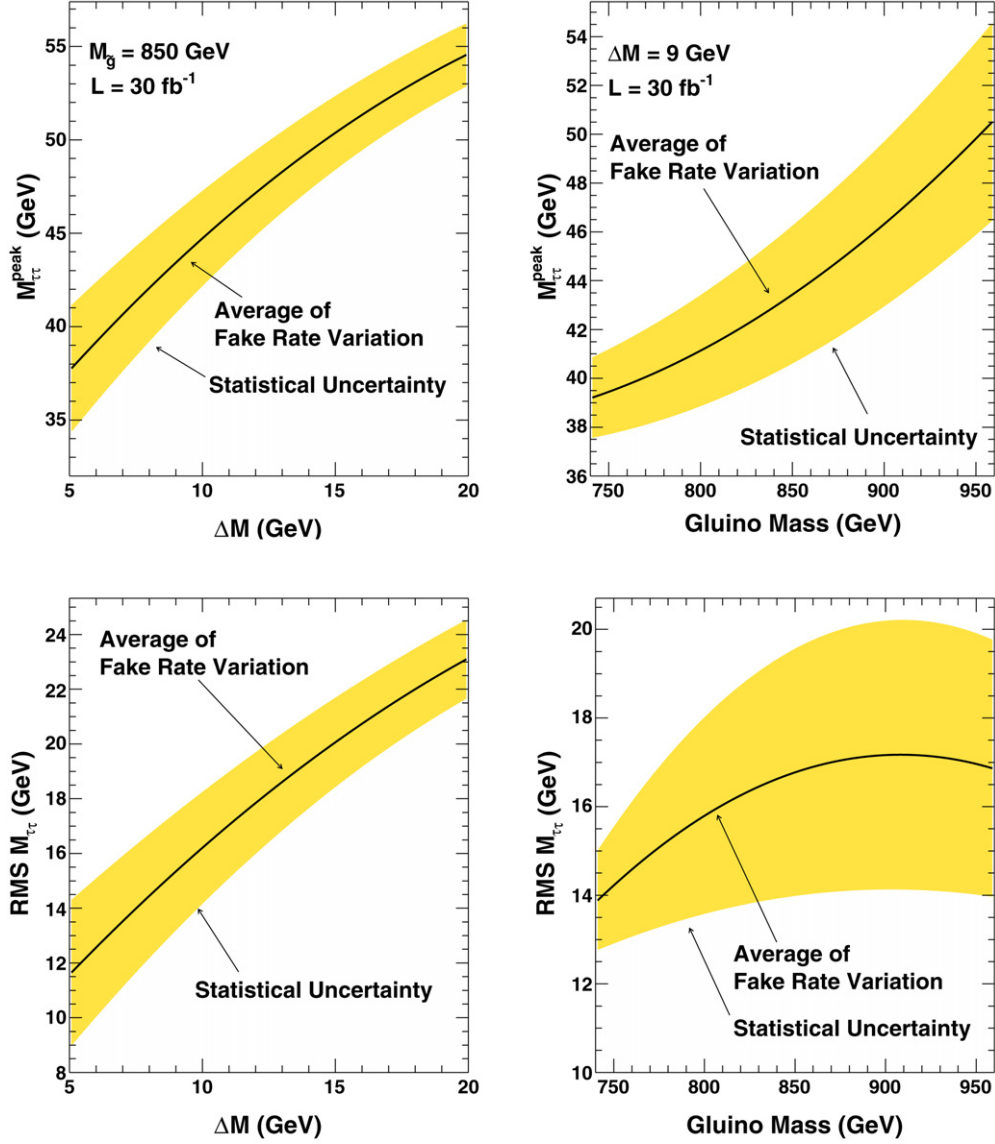


Fig. 4. The upper plots show $M_{\tau\tau}^{\text{peak}}$ as a function of ΔM (left) and $M_{\tilde{g}}$ (right). The $M_{\tau\tau}^{\text{peak}}$ increases strongly with both increasing ΔM and $M_{\tilde{g}}$. The lower plots show the RMS of the $M_{\tau\tau}$ distribution as a function ΔM (left) and $M_{\tilde{g}}$ (right). The statistical uncertainty is significantly larger than the uncertainty due to fake rate variation and is taken here normalized to expectations for 30 fb^{-1} . Each is large compared to the effects of jet resolution (see footnote 2). Note that a mass measurement is not possible for ΔM values less than 6 GeV due to the inability to form a mass peak even at high luminosities.

in order to make a measurement, we find that for values of $\Delta M \gtrsim 8 \text{ GeV}$, we require just less than 10 fb^{-1} for 3σ significance. For ΔM below 6 GeV, no amount of luminosity suffices to reach the 3σ level since the third τ is not energetic enough to be observed, and no $M_{\tau\tau}^{\text{peak}}$ can be constructed.

Fig. 6 shows the expected uncertainty on ΔM as a function of ΔM and the expected percent uncertainty on ΔM and $M_{\tilde{g}}$ as functions of luminosity for $\Delta M = 9 \text{ GeV}$ and $M_{\tilde{g}} = 850 \text{ GeV}$. Note that we have used the 1σ intersecting lines as they conservatively overestimate our systematic error. We find that for $\mathcal{L} = 30 \text{ fb}^{-1}$ we can measure ΔM to $\sim 15\%$ and $M_{\tilde{g}}$ to $\sim 6\%$. For 10 fb^{-1} , these uncertainties become 20% and 9% respectively. It is important to note again, however, that our determination of $M_{\tilde{g}}$ is not a direct measurement, but a determination of a parameter in our model, in some sense, the SUSY mass

scale of the model. It will need to be compared to a direct $M_{\tilde{g}}$ measurement, when one becomes available. If the two results were consistent, it would be a consistency check of the gaugino universality of the mSUGRA model and that we are indeed in the co-annihilation region.

If we assume an independently measured $M_{\tilde{g}}$, as in previous analyses [11,13], our two observables can be considered to be two independent measurements of ΔM that can be compared and combined for further testing of the model. We assume here that $M_{\tilde{g}} = 850 \text{ GeV}$ and has been measured to 5%, and we incorporate this uncertainty into our ΔM measurement as a systematic uncertainty. To do this, we determine the variation in our observables from the expected values at a fixed ΔM but with $M_{\tilde{g}}$ varying by 5%. We then propagate these variations using parameterizations of our observables with $M_{\tilde{g}}$

fixed as in [13]. The results are shown in the top plots of Fig. 7. We see that for both methods the systematic uncertainty on the gluino mass clearly dominates. Combining the two results using $\sigma_{\text{combined}} = 1/\sqrt{\sigma_{\text{counting}}^{-2} + \sigma_{\text{mass}}^{-2}}$ we find that with $\mathcal{L} = 30 \text{ fb}^{-1}$ ΔM can be measured to 12% at our 9 GeV mass point. The mass method is always slightly worse than the counting method but does help improve the combined uncertainty. The full results are shown in the bottom left and bottom right of Fig. 7. Alternatively, one could use our two observables to study ΔM and gaugino unification (i.e. k or k_1 in Eq. (3)). This is under study.

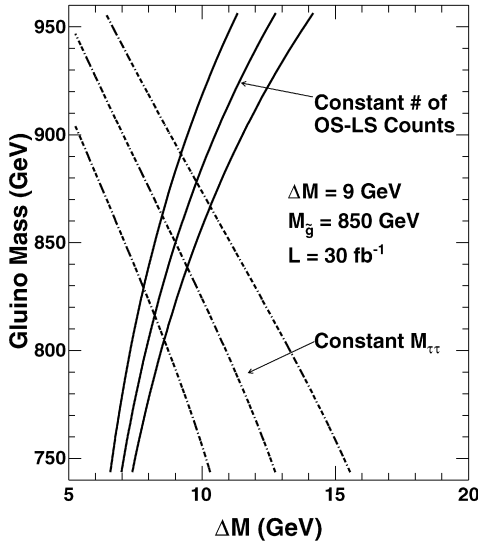


Fig. 5. The contours of constant $N_{\text{OS-LS}}$ and $M_{\tau\tau}^{\text{peak}}$ for $\Delta M = 9 \text{ GeV}$, $M_{\tilde{g}} = 850 \text{ GeV}$, and $\mathcal{L} = 30 \text{ fb}^{-1}$. The middle lines are the central values while the outer lines show the 1σ uncertainty on the measurements. The region defined by the outer four lines indicates the 1σ region for the ΔM and $M_{\tilde{g}}$ measurements in Fig. 6.

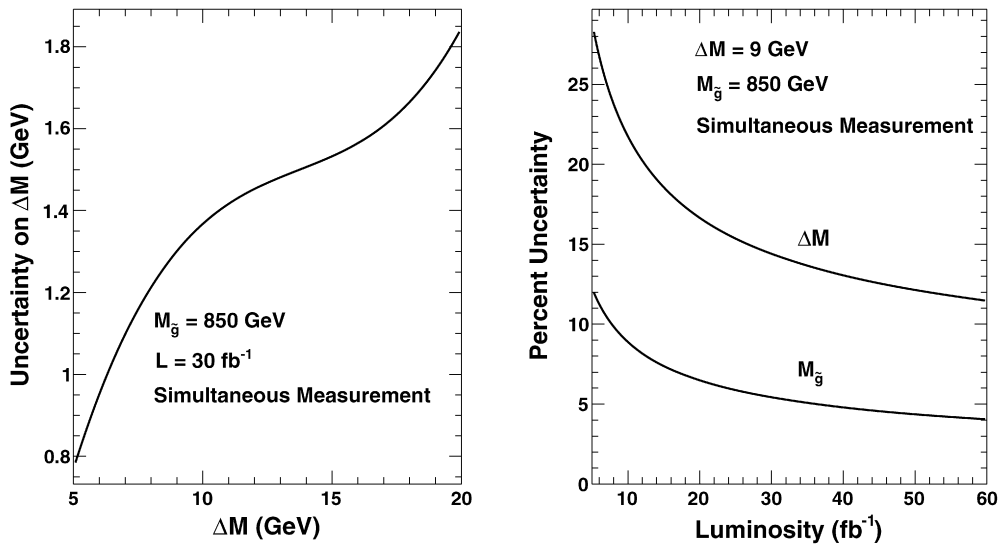


Fig. 6. The expected uncertainty on ΔM and $M_{\tilde{g}}$ for the simultaneous measurement method. The plot on the left shows the uncertainty on ΔM as a function of ΔM . The plot on the right shows the percent uncertainty in ΔM and $M_{\tilde{g}}$ as functions of luminosity for $\Delta M = 9 \text{ GeV}$ and $M_{\tilde{g}} = 850 \text{ GeV}$. Even at high luminosities, the uncertainties on both ΔM and $M_{\tilde{g}}$ continue to improve and continue to be statistics limited.

4. Conclusions

The co-annihilation region is a difficult scenario to measure at the LHC because of the large number of soft, final state taus. Indeed, previous studies of high $\tan\beta$ scenarios have likely overestimated their ability to establish that we are in this region by concentrating on large ΔM . In this Letter, we present the first study of simultaneously measuring ΔM and $M_{\tilde{g}}$ at the LHC with a precision that would establish the co-annihilation region and show that the $\tilde{\chi}_1^0$ is the dark matter particle. We use the inclusive $3\tau + \text{jet} + \cancel{E}_T$ final state, and because this channel is nearly background free after selection cuts for $\Delta M \gtrsim 6 \text{ GeV}$, we are able to form two separate observables: the number of signal events (a $\tilde{\chi}_2^0$ cross-section measurement equivalent) and $M_{\tau\tau}^{\text{peak}}$. Both vary with ΔM and $M_{\tilde{g}}$ allowing the simultaneous measurement of both. Using mSUGRA scenario assumptions we find that with 10 fb^{-1} we can measure ΔM to 20% and $M_{\tilde{g}}$ to 9% for the example point of $\Delta M = 9 \text{ GeV}$ and $M_{\tilde{g}} = 850 \text{ GeV}$; with 30 fb^{-1} we can measure them to 15% and 6% respectively. While our sensitivity to measuring ΔM at the LHC is not as good as that expected at the ILC, it is quite comparable and should be available much sooner. For high luminosity, if an independent gluino mass measurement were performed at LHC, with a 5% precision, we have found that it is possible to measure ΔM to 12% for our baseline point; similarly assuming ΔM , the measurement of some other parameter of the theory is possible. We also note that we have made no attempt to optimize these results, indicating that with actual data from the detector, we will likely be able to improve our cuts, leading to a more precise measurement or a lower luminosity needed for the same sensitivity. We have confirmed that efficient τ identification down to an E_T of 20 GeV is crucial for this analysis as in the 2τ analysis [13]. Further, we expect that this analysis and other 2τ analyses could be used to com-

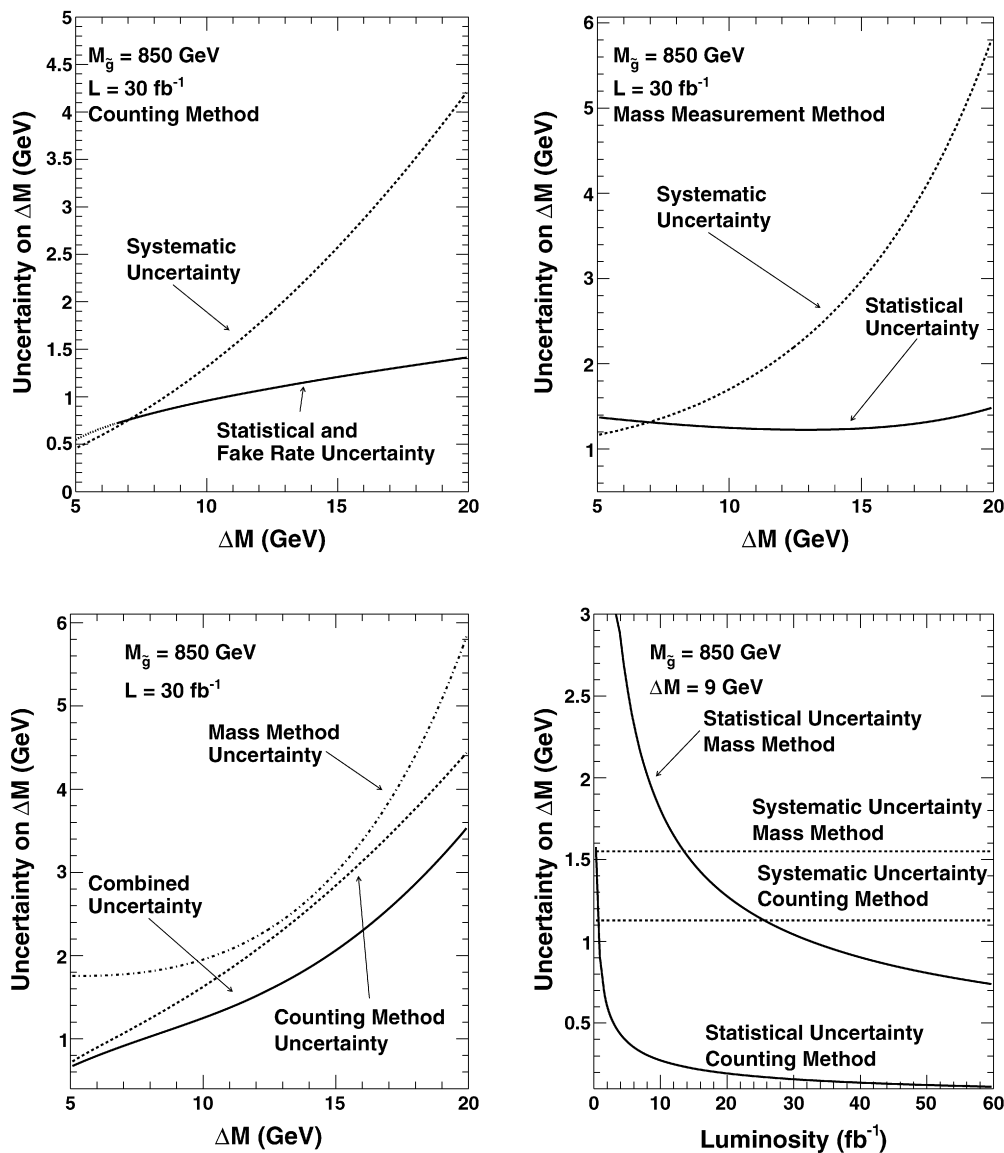


Fig. 7. With the assumption that $M_{\tilde{g}}$ is measured elsewhere to 5%, we use the N_{OS-LS} and $M_{\tau\tau}^{\text{peak}}$ values to make two independent measurements of ΔM , which can be combined to produce a more accurate measurement. The top plots show the sources of uncertainty for the counting (left) and the mass (right) methods. In both cases, the systematic uncertainty on the gluino mass dominates the measurement. The bottom plots show the combined results as a function of ΔM (left) and luminosity (right). We note that both methods are systematics limited by $\mathcal{L} = 10$ fb $^{-1}$.

plement each other in the establishment of a co-annihilation signal at the LHC, and perhaps be combined to produce a more accurate measurement, or help confirm SUGRA GUT assumptions. Finally, an analysis of this type can be applied to other SUGRA models provided they have a co-annihilation region and do not suppress the production of the $\tilde{\chi}_2^0$ particles.

Acknowledgements

This work was supported in part by the Texas A&M Graduate Merit Fellowship program, DOE grant DE-FG02-95ER40917, and NSF grant DMS 0216275. We would like to thank A. Gurrola for useful discussions.

References

- [1] D.Z. Freedman, P. Van Nieuwenhuisen, S. Ferrara, Phys. Rev. D 13 (1976) 3214;
S. Deser, B. Zumino, Phys. Lett. B 65 (1976) 369.
- [2] A.H. Chamseddine, R. Arnowitt, P. Nath, Phys. Rev. Lett. 49 (1982) 970.
- [3] R. Barbieri, S. Ferrara, C.A. Savoy, Phys. Lett. B 119 (1982) 343;
L. Hall, J. Lykken, S. Weinberg, Phys. Rev. D 27 (1983) 2359;
P. Nath, R. Arnowitt, A.H. Chamseddine, Nucl. Phys. B 227 (1983) 121;
For a review, see P. Nilles, Phys. Rep. 100 (1984) 1.
- [4] U. Amaldi, W. de Boer, H. Furstenu, Phys. Lett. B 260 (1991) 447.
- [5] J. Ellis, K. Olive, Y. Santoso, V. Spanos, Phys. Lett. B 565 (2003) 176;
R. Arnowitt, B. Dutta, B. Hu, hep-ph/0310103;
H. Baer, C. Balazs, A. Belyaev, T. Krupovnickas, X. Tata, JHEP 0306 (2003) 054;
B. Lahanas, D.V. Nanopoulos, Phys. Lett. B 568 (2003) 55;
U. Chattopadhyay, A. Corsetti, P. Nath, Phys. Rev. D 68 (2003) 035005;

- E. Baltz, P. Gondolo, JHEP 0410 (2004) 052;
B.C. Allanach, C.G. Lester, Phys. Rev. D 73 (2006) 015013;
A. Djouadi, M. Drees, J.-L. Kneur, JHEP 0603 (2006) 033.
- [6] WMAP Collaboration, D.N. Spergel, et al., Astrophys. J. Suppl. 148 (2003) 175.
- [7] K. Griest, D. Seckel, Phys. Rev. D 43 (1991) 3191.
- [8] ALEPH Collaboration, DELPHI Collaboration, L3 Collaboration, OPAL Collaboration, LEP Working Group for Higgs Boson Searches, G. Abbiendi, et al., Phys. Lett. B 565 (2003) 61;
Particle Data Group, S. Eidelman, et al., Phys. Lett. B 592 (2004) 1.
- [9] M. Alam, et al., Phys. Rev. Lett. 74 (1995) 2885.
- [10] Muon $g-2$ Collaboration, G. Bennett, et al., Phys. Rev. Lett. 92 (2004) 161802;
S. Eidelman, Talk at ICHEP 2006, Moscow, Russia;
J.P. Miller, E. de Rafael, B.L. Roberts, hep-ph/0703049.
- [11] V. Khotilovich, R. Arnowitt, B. Dutta, T. Kamon, Phys. Lett. B 618 (2005) 182.
- [12] I. Hinchliffe, F.E. Paige, Phys. Rev. D 61 (2000) 095011.
- [13] R. Arnowitt, B. Dutta, T. Kamon, N. Kolev, D. Toback, Phys. Lett. B 639 (2006) 46.
- [14] CDF Collaboration, D. Acosta, et al., Phys. Rev. Lett. 92 (2004) 051803.
- [15] F. Paige, S. Protopescu, H. Baer, X. Tata, hep-ph/0312045. We use ISAJET version 7.64 without TAUOLA.
- [16] PGS is a parameterized detector simulator. We used version 3.2 (see <http://www.physics.ucdavis.edu/~conway/research/software/pgs/pgs4-general.htm>).
- [17] CDF Collaboration, D. Acosta, et al., Phys. Rev. Lett. 95 (2005) 131801.
- [18] F. Heinemann, hep-ex/0406056, 2004.
- [19] Systematic uncertainties on event rates can arise from uncertainties in the structure functions, QCD corrections, tau tagging efficiency etc. The two most relevant guideposts from the Tevatron are a multitau cross section measurement of $\sigma \cdot \text{Br}(Z \rightarrow \tau\tau) = 264 \pm 23(\text{stat}) \pm 14(\text{syst}) \pm 15(\text{lumi})$ pb (CDF Collaboration, A. Abulencia et al., FERMILAB-PUB-07-025E, Phys. Rev. D, in press) and large-mass-strong-production measurements of $\sigma(t\bar{t}) = 7.3 \pm 0.5(\text{stat}) \pm 0.6(\text{syst})$ pb, E. Shabalina for CDF and D0 Collaborations, hep-ex/0605045. In both cases, as in ours, the systematics ($\sim 10\%$ or less) tend to be smaller than the statistical uncertainty.